JOURNAL OF NATURAL PRODUCTS

Article

Cite This: J. Nat. Prod. XXXX, XXX, XXX−XXX

pubs.acs.org/jnp

Ribocyclophanes A−E, Glycosylated Cyclophanes with Antiproliferative Activity from Two Cultured Terrestrial Cyanobacteria

Daniel S. May,[†,∥] Hahk-Soo Kang,[†,§,∥] Bernard D. Santarsiero,[‡] Aleksej Krunic,[†] Qi Shen,[†] Joanna E. Burdette,[†] Steven M. Swanson,[†,⊥] and Jimmy Orjala*[,†]

[†]Department of Medicinal Chemistry and Pharmacognosy, University of Illinois at Chicago, Chicago, Illinois 60612, United States

[‡]Center for Biomolecular Sciences, University of Illinois at Chicago, Chicago, Illinois 60607, United States

[⊥]School of Pharmacy, University of Wisconsin at Madison, Madison, Wisconsin 53705, United States

Supporting Information

ABSTRACT: The cell extracts of two cultured freshwater *Nostoc* spp., UIC 10279 and UIC 10366, both from the suburbs of Chicago, showed antiproliferative activity against MDA-MB-231 and MDA-MB-435 cancer cell lines. Bioassay-guided fractionation led to the isolation of five glycosylated cylindrocyclophanes, named ribocyclophanes A−E (**1**−**5**) and cylindrocyclophane D (**6**). The structure determination was carried out by HRESIMS and 1D and 2D NMR analyses and confirmed by single-crystal X-ray crystallography. The structures of ribocyclophanes A−E (**1**−**5**) contain a β-D-ribopyranose glycone in the rare $^1C_4$ conformation. Among isolated compounds, ribocyclophane D (**4**) showed antiproliferative activity against MDA-MB-435 and MDA-MB-231 cancer cells with an IC_{50} value of less than 1 μM.

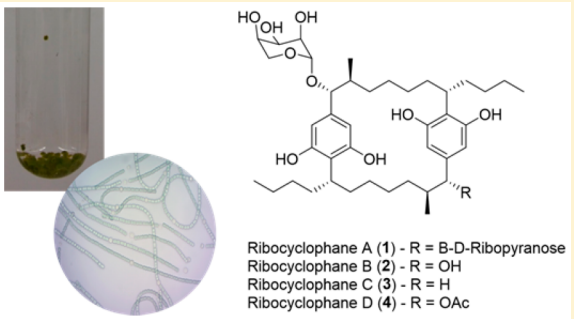

Polyketides (PKs), one of the largest families of natural products, are not commonly found in cyanobacteria compared to other major natural products families, such as nonribosomal peptides (NRPs) and PK−NRP hybrids.[1−3] However, [7.7]paracyclophanes represent a family of cyanobacterial polyketides that has been found in heterocyst-forming cyanobacteria of the order Nostocales.[4−11] The 22-membered [7.7]paracyclophane core structure, possessing a C_2 axis of symmetry, has been shown to be produced by dimerization of two halogenated alkyl-resorcinol units made by a type I/type III polyketide synthase hybrid.[12−14] The alkyl-resorcinol units, termed cylindrofridins, were isolated by Preisitsch et al. and proposed as biosynthetic intermediates.[15] The identification of the biosynthetic intermediates by Nakamura et al. confirmed the biosynthetic origin of these alkyl-resorcinol units as well as their dimerization.[13,14,16] The core [7.7]paracyclophane structure is further modified by tailoring steps such as methylation, acetylation, carbamate formation, glycosylation, and/or halogenation, to generate diverse structural variants.[17] Cyanobacterial cyclophanes have been shown to possess a broad range of biological activities, including antibacterial, antifungal, and cytotoxic activities.[6−11]

Several *Nostoc* spp. from the University of Illinois at Chicago (UIC) cyanobacterial library have been identified to produce [7.7]paracyclophanes. Chlorinated cylindrocyclophanes were obtained from a *Nostoc* sp. (UIC 10022A).[7] These chlorinated cyclindrocyclophanes exhibited 20S proteasome-inhibitory activity and cytotoxicity against several cancer cell lines. Carbamidocyclophanes F and G were reported from UIC 10274, containing terminal chlorines as well as an uncommon carbamate moiety.[10] In addition, the isolation of merocyclophanes A and B from a *Nostoc* sp. (UIC 10062) from Grand Mere State Park in Michigan was reported, as well as merocyclophanes C and D from the extract of UIC 10110, a *Nostoc* sp. from Colorado. Merocyclophanes A−D featured a new [7.7]paracyclophane carbon skeleton characterized by the presence of branched methyls at α positions (C-1/14).[8,11] The extract of a cultured *Nostoc* sp. (UIC 10279), obtained from a sample collected in the southwest suburbs of Chicago, displayed antiproliferative activity against the human melanoma cancer cell line MDA-MB-435. HPLC-based activity profiling followed by LCMS and ^{1}H NMR-based dereplication suggested the presence of three glycosylated cyclophanes as active metabolites. Concurrently, a second *Nostoc* sp. (UIC 10366), obtained from a collection in the northwestern suburbs of Chicago, also displayed antiproliferative activity against MDA-MB-435 cancer cells. LCMS and ^{1}H NMR-based dereplication also suggested the presence of glycosylated cyclophanes similar to UIC 10279, including one unique to UIC 10366. During

Special Issue: Special Issue in Honor of Susan Horwitz

Received: November 10, 2017

DOI: 10.1021/acs.jnatprod.7b00954
J. Nat. Prod. XXXX, XXX, XXX−XXX

isolation, a fifth minor compound was identified from UIC 10366. Herein, we report the isolation, structure determination, and antiproliferative activities of five glycosylated cyanobacterial [7.7]paracyclophanes, named ribocyclophanes A–E (**1**–**5**).

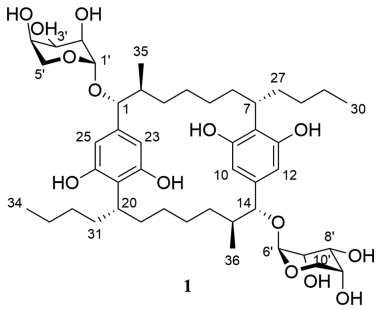

1

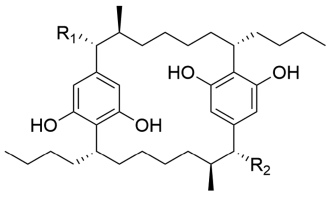

2 R_1 = Ribose, R_2 = OH
3 R_1 = Ribose, R_2 = H
4 R_1 = Ribose, R_2 = OAc
6 R_1 = OAc, R_2 = OAc

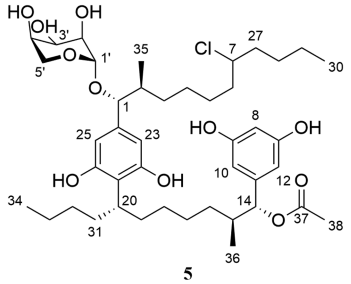

5

RESULTS AND DISCUSSION

Strain UIC 10279 was obtained from a sample collected southwest of Chicago near the suburb of Joliet, Illinois, while strain UIC 10366 was obtained from a sample collected near Elgin, Illinois, a suburb northwest of Chicago. The strains were both designated as *Nostoc* sp. based on morphological and 16S rRNA gene sequence analysis (Supporting Information, S1 and S2). Each strain was cultured in Z media,[18] and the freeze-dried cells were extracted with a mixture of CH_2Cl_2 and MeOH (1:1, v/v). The resulting extracts displayed antiproliferative activity against the MDA-MB-435 cancer cell line. Both extracts were fractionated using Diaion HP-20 resin with an increasing amount of iPrOH in H_2O. Fractions eluting at 50% and 60% iPrOH showed antiproliferative activity for both strains. To facilitate the identification of potentially active compounds, the active fractions were subjected to our HPLC-based activity profiling that combines HPLC-based fractionation in a 96-well plate with the cell-based activity assay. Three active compounds were identified in each strain. Dereplication of the active fractions of UIC 10279 by LC-MS and ^{1}H NMR spectroscopy indicated the presence of glycosylated cyclophanes with molecular weights of 848, 716, and 700 Da. Dereplication of the active peaks of UIC 10366 by LC-MS and ^{1}H NMR spectroscopy indicated the presence of the previously reported cylindrocyclophane D as well as two potentially new glycosylated cyclophanes with molecular weights of 848 and 758 Da.[4] Active fractions for each strain were subjected to reversed-phase HPLC to yield six pure compounds between the two extracts. During isolation from the extract of UIC 10366, a low abundance compound, ribocyclophane E (**5**), was also obtained. Ribocyclophanes A (**1**, 0.5%), B (**2**, 0.1%), and C (**3**, 0.3%) were isolated from UIC 10279, and ribocyclophanes A (**1**, 0.5%), D (**4**, 0.5%), and E (**5**, < 0.1%) as well as the known compound cylindrocyclophane D (**6**, 0.2%) were isolated from UIC 10366.

Ribocyclophane A (**1**), a white amorphous powder obtained from UIC 10279, displayed a deprotonated molecule at m/z 847.4895 ($[M - H]^-$) in the HRESIMS analysis, corresponding to a molecular formula of $C_{46}H_{71}O_{14}$. The ^{1}H NMR spectrum of **1** showed signals characteristic of cylindrocyclophanes with two singlet aromatic protons (H-10/23, δ_H 6.19; H-12/25, δ_H 6.09), benzylic doublet and multiplet methines (H-1/14, δ_H 3.65; H-7/20, δ_H 3.16), shielded diastereotopic methylenes (H_2-3/16 and H_2-5/18, δ_H 0.5–1.0), and a doublet methyl (H_3-35/36, δ_H1.05). Only half the number of signals were observed in the ^{1}H and ^{13}C NMR spectra, as indicated by the molecular formula, suggesting the presence of an element of symmetry in **1**. The ^{1}H NMR spectrum of **1** showed an additional set of proton signals adjacent to oxygen (δ_H 3.0–4.0) and an anomeric proton (δ_H 4.85) compared to those observed for the cylindrocyclophanes, suggesting the presence of a glycoside moiety in **1**. The structure and position of a sugar moiety were determined by 2D NMR analysis. Sequential COSY correlations from the anomeric proton H-1′/6′ (δ_H 4.85) to the diastereotopic methylene protons H_2-5′/10′ (δ_H 3.19 and 3.30) via three hydroxylated methine protons, H-2′/7′ (δ_H 3.73), H-3′/8′ (δ_H 3.70), and H-4′/9′ (δ_H 3.59), together with an HMBC correlation from H_2-5′/10′ to C-1′/6′, indicated the sugar moiety to be a pentopyranose (Figure 1). The HMBC correlation observed from the anomeric protons H-1′/6′ to C-1/14 established the linkage between the pentopyranose and the cylindrocyclophane aglycone.

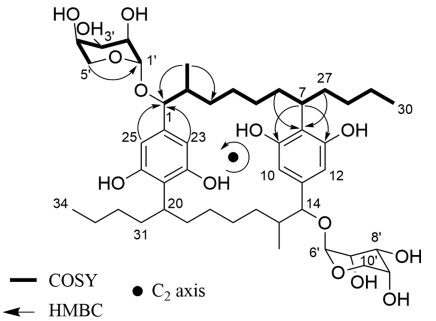

Figure 1. Key 2D NMR correlations used for the determination of the structure of ribocyclophane A (**1**).

To determine the relative configuration of the sugar moiety, $^3J_{HH}$ analysis and an NOE experiment were initially attempted. The small $^3J_{HH}$ value (1.8 Hz), observed between H-1′/6′ and H-2′/7′, indicated that these two protons are in an either ax–eq or eq–eq relationship. The $^3J_{HH}$ values between H-2′/7′, H-3′/8′, and H-4′/9′ could not be measured directly from the ^{1}H

DOI: 10.1021/acs.jnatprod.7b00954
J. Nat. Prod. XXXX, XXX, XXX–XXX

NMR spectrum due to the broad signals observed; however, the broad line shapes of NMR signals observed for all of the signals indicated small $^3J_{HH}$ values between these protons. In addition, no NOE correlation was observed between H-1′/6′ and H-3′/8′ and between H-2′/7′ and H-4′/9′, complicating the determination of the relative configuration for the sugar moiety. To unambiguously determine the $^3J_{HH}$ values of the glycone moiety, spin simulation was performed using Spinworks. The $^3J_{HH}$ values measured using spin simulation were 3.0 (H-2′/7′ and H-3′/8′), 3.0 (H-3′/8′ and H-4′/9′), 1.2 (H-4′/9′ and H-5′a/10′a), and 2.4 Hz (H-4′/9′ and H-5′b/10′b), respectively. These small J values clearly demonstrated that all the protons are in ax−eq or eq−eq relationships, thus suggesting β-D-ribopyranose ($^1C_4$), β-L-ribopyranose ($^4C_1$), β-D-xylopyranose ($^1C_4$), or β-L-xylopyranose ($^4C_1$) as a possible glycone moiety. All of these possible sugar moieties adopt thermodynamically unfavorable conformations where three or all four oxygen atoms are in axial positions. To unambiguously disclose the relative configuration of the sugar moiety as well as its spatial conformation, single-crystal X-ray crystallographic analysis was carried out using a crystal obtained from a mixture of EtOH and H_2O (1:1) by slow evaporation. The crystal structure (Figure 2) of **1** revealed that the relative configuration

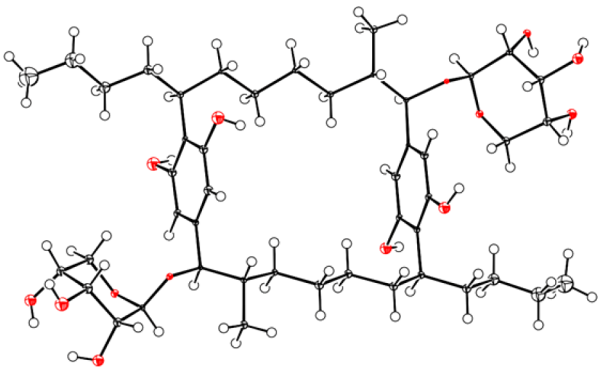

Figure 2. ORTEP drawing of ribocyclophane A (**1**).

of the glycone moiety is a β-ribopyranose where oxygen atoms at C-1′, C-2′, and C-4′ were axially positioned. The absolute configuration of **1** was determined by measuring the optical rotation of the glycone moiety and electronic circular dichroism (ECD) analysis of the aglycone moiety, each liberated by acid hydrolysis (1 N HCl). The negative rotation ($[\alpha]_D$ −9) observed for the glycone moiety indicated the absolute configuration to be a β-D-ribopyranose with $^1C_4$ conformation (Figure 2). Negative Cotton effects observed at 230 and 280 nm for the aglycone moiety are identical to those observed for cylindrocyclophane A, indicating the same absolute configuration.[6] The potential energy of a $^1C_4$ conformation is approximately 4 times higher than that of a $^4C_1$ conformation for β-D-ribopyranose.[19] The adoption of a thermodynamically unfavorable conformation for the glycone moiety could be rationalized by a favored spatial arrangement to avoid a steric interaction between the algycone and glycone moieties in the overall structure (Figure 3). The β-D-ribopyranose glycone with the preferred $^4C_1$ conformation occupies a much larger spatial volume than that with a $^1C_4$ conformation, creating a steric effect with the aromatic ring and branched methyl of the cylindrocyclophane aglycone. This steric effect forces the sugar moiety into a $^1C_4$ conformation, and the adoption of a $^1C_4$ conformation increases the overall stability of **1** by reducing the

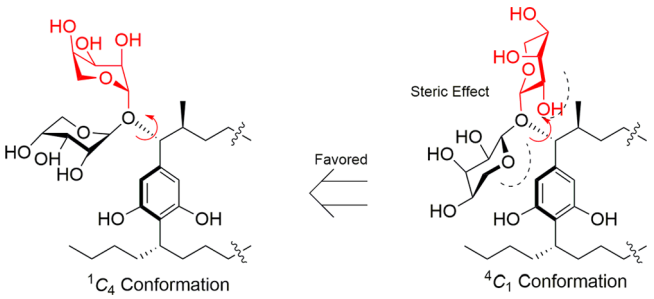

Figure 3. β-D-Ribopyranose glycone adopts the less favorable $^1C_4$ conformation to avoid steric interactions with the cylindrocyclophane aglycone moiety.

spatial volume of the glycone moiety. The selection of the unfavorable $^1C_4$ conformation is also supported by the anomeric effect, in which heteroatom substituents preferentially assume an axial orientation when adjacent to a heteroatom within a ring. The glycone moiety of **1** obtained from UIC 10366 was found to have the same negative specific rotation and identical ^{1}H NMR signals to those observed for **1** from UIC 10279, suggesting that the glycone produced by UIC 10366 is also a β-D-ribopyranose. The crystal structure of **1** allowed the assignment of the stereocenters of the cylindrocyclophane aglycone as 1*R*, 2*S*, 7*R*, 14*R*, 15*S*, 20*R*, which are identical to those reported for cylindrocyclophane A.

Ribocyclophane B (**2**) was obtained as a white amorphous powder from UIC 10279, and HRESIMS analysis (m/z 715.4477 $[M - H]^-$) suggested the molecular formula of **2** to be $C_{41}H_{64}O_{10}$. The ^{1}H NMR spectrum of **2** showed an overall signal distribution pattern similar to that observed for **1**. The appearance of four singlet aromatic (δ_H 6.07, 6.09, 6.20, and 6.24) and two doublet methyl (δ_H 1.05 and 1.06) signals indicated the structure of **2** to be nonsymmetrical. The integration of each signal of the glycone moiety corresponded to that of one aromatic proton signal of the aglycone moiety, suggesting the presence of only one sugar moiety in **2**. The newly appearing signal of H-14 (δ_H 3.74) compared to **1**, together with the mass difference of 132 between **2** and **1**, demonstrated that one of the glycoside moieties in **1** was replaced by a hydroxy group in **2**. The ECD spectrum of **2** showed positive Cotton effects at 221 and 275 nm, identical to those observed for **1**, suggesting the same absolute configuration for **2**.

Ribocyclophane C (**3**) was obtained as a white amorphous powder from UIC 10279. HRESIMS analysis (m/z 699.4533 $[M - H]^-$) suggested the molecular formula of **3** as $C_{41}H_{64}O_9$. The ^{1}H NMR spectrum of **3** closely resembled that of **2**, and four aromatic and two doublet methyl signals were observed, thus indicating the structure of **2** to be nonsymmetrical due to the presence of one glycone moiety. The notable difference was the replacement of an oxygenated methine proton H-14 in **2** by diastereotopic methylene protons (δ_H 1.81 and 2.61) in **3**. This, together with the 16 mass difference between **2** and **3**, which corresponded to one oxygen atom, suggested the absence of the hydroxy group at C-14. This was confirmed by NMR analysis (Table 2), demonstrating the structure of **3** to be the deoxygenated analogue of **2**. The positive Cotton effects observed at 222 and 274 nm indicated the same absolute configuration of **3** as determined for **2**.

Ribocyclophane D (**4**) was obtained as a white amorphous powder from UIC 10366. HRESIMS analysis (m/z 757.4489

DOI: 10.1021/acs.jnatprod.7b00954
J. Nat. Prod. XXXX, XXX, XXX−XXX

Table 1. NMR Spectroscopic Data of Ribocyclophane A (1) in MeOH-d_4

no.	δ_C,[a] type	δ_H,[b] mult. (J in Hz)	COSY[b]	HMBC[b]
1/14	90.1, CH	3.65, d (12.2)	2/15	2/15, 3/16, 10/23, 11/24, 12/25, 35/36, 1′/6′
2/15	41.8, CH	1.65, m	1/14, 3/16, 35/36	NA[c]
3/16	34.9, CH_2	0.66, m	2/15, 4/17	NA[d]
		0.75, m		
4/17	30.0, CH_2	0.82, m	3/16, 5/18	NA[c]
		1.44, m		
5/18	30.9, CH_2	0.71, m	4/17, 6/19	NA[d]
		0.96, m		
6/19	35.5, CH_2	1.32, m	5/18, 7/20	4/17, 5/18, 7/20, 27/31
		2.03, ddd (4.2)		
7/20	37.0, CH	3.16, m	6/19, 27/31	5/18, 6/19, 8/21, 9/22, 13/26, 27/31, 28/32
8/21	117.9, C			
9/22	158.9, C			
10/23	105.5, CH	6.19, s		1/14, 12/25, 8/21, 9/22
11/24	142.1, C			
12/25	109.3, CH	6.09, s		1/14, 10/23, 8/21, 13/26
13/26	157.1, C			
27/31	34.8, CH_2	1.47, m	7/20, 28/32	6/19, 7/20, 8/21, 28/32, 29/33
		1.95, m		
28/32	31.9, CH_2	1.04, m	27/31, 29/33	NA[d]
		1.17, m		
29/33	24.0, CH_2	1.18, m	28/32, 30/34	NA[d]
		1.28, m		
30/34	14.8, CH_3	0.79, t (7.2)	29/33	28/32, 29/33
35/36	16.7, CH_3	1.05, d (6.0)	2/15	1/14, 2/15, 3/16
1′/6′	104.6, CH	4.85, d (1.8)	2′/7′	1/14, 5′/10′, 2′/7, 3′/8′
2′/7′	72.8, CH	3.73, d (1.8, 3.0)	1′/6′, 3′/8′	NA[c]
3′/8′	66.9, CH	3.70, t (3.0)	2′/7′, 4′/9′	NA[c]
4′/9′	71.6, CH	3.59, ddd (2.4, 3.0)	3′/8′, 5′/10′	NA[c]
5′/10′	65.6, CH_2	3.19, dd (12.6, 2.4)	4′/9′	1′/6′, 3′/8′, 4′/9′
		3.30, dd (12.6)		

[a]Assigned from the DEPT-Q spectrum acquired at 226 MHz. [b]Recorded at 600 MHz. [c]No signals were observed. [d]Could not be assigned due to the signal overlap.

$[M - H]^-$) suggested the molecular formula of **4** to be $C_{43}H_{66}O_{11}$. The ^{1}H NMR spectrum of **4** was similar to that of **2** and **3**, suggesting the compound was nonsymmetrical due to differing moieties on the cylindrocyclophane scaffold. The difference in molecular formula between **2** and **4** suggested the presence of an acetate group. The presence of a singlet at δ_H 2.0 in the ^{1}H NMR spectrum and signals at δ_C 21.3 and δ_C 172.6 in the ^{13}C NMR spectrum confirmed the presence of an acetate moiety. HMBC correlations from H-14 to C-37 confirmed the placement of the acetate moiety α to the resorcinol core. The positive Cotton effects observed at 222 and 273 nm indicated the same absolute configuration as all previously described [7.7]paracyclophanes.

Ribocyclophane E (**5**) was obtained as a minor component from UIC 10366 during the isolation of **4**. HRESIMS analysis showed an isotopic pattern consistent with the presence of one chlorine atom and suggested a molecular formula of $C_{43}H_{67}ClO_{11}$ (m/z 793.9098 $[M - H]^-$ and 795.9101 $[M - H]^-$ in a 3:1 ratio). Comparing the ^{1}H NMR spectrum to the spectra for **1**–**4** indicated **5** to be structurally different. The ^{1}H NMR spectrum of **5** was more similar to the ^{1}H NMR spectra of the cylindrofridins published by Preisitsch et al.[15] NMR analysis allowed the assignment of two aliphatic chains as well as a ribose. The signal at δ_H 3.83 indicated a proton adjacent to a halogen, suggesting the presence of the chlorine atom on one of the aliphatic chains. HSQC and ^{13}C spectra confirmed the presence of the chlorine, with the signal at δ_H 3.83 correlating to C-7 at δ_C 65.1. COSY correlations from H-7 to H-6 and H-27 confirmed the placement of the chlorine along the aliphatic chain. The presence and positions of two resorcinol-like groups were deduced by HMBC correlations from H-23/25 to C-1 and likewise from H-10/12 to C-14, H-20 to C-22/26, and H-31/19 to C-21. No correlations were observed from H-7 to C-9/13 or H-6/27 to C-8, as would be present in other [7.7]-paracyclophane HMBC spectra. This is consistent with cylindrofridin-like structures that are linear. HMBC correlation from H-1 to C-1′ confirmed the position of the ribose, and a correlation from H-14 to C-37, along with the strong singlet signal at δ_H 2.07, suggested the presence of an acetate moiety. The Cotton effects observed at 222 and 274 nm indicated the same absolute configuration as the previously described cylindrofridins and [7.7]paracyclophanes.[15] We were unable to establish the configuration of the stereogenic center at C-7.

Ribocyclophanes A–D (**1**–**4**) are glycosylated analogues of the cyclindrocyclophanes. Ribocyclophane E (**5**) is a glycosylated analogue of the cylindrofridins and a likely biosynthetic intermediate of **4**. A notable structural feature of **1**–**4** is the presence of a β-D-ribopyranose glycone moiety linked to the benzoyl carbon of the cylindrocyclophane aglycone. This glycone moiety exclusively adopted the thermodynamically unfavorable $^1C_4$ conformation in which three oxygen atoms are in axial positions and one oxygen atom is in an equatorial position. The crystal structure of **1** showed that no hydrogen bonding is involved between the glycone and aglycone moieties to favor the shift of conformational equilibrium toward the $^1C_4$ conformation. This suggested that an avoidance of steric crowding between the β-D-ribopyranose glycone and the cylindrocyclophane aglycone is likely to be the major driver of the adoption of the $^1C_4$ conformation.

Ribocyclophanes A–E (**1**–**5**) and cylindrocyclophane D (**6**) were tested for their antiproliferative activity against MDA-MB-231 and MDA-MB-435 cancer cell lines. Ribocyclophane D (**4**) showed the strongest activity among six compounds with IC_{50} values of less than 1 μM in both cell lines (IC_{50} 0.8 and 0.6 μM, respectively), whereas moderate activity was observed for ribocyclophane C (**3**) (IC_{50} 1.2 and 1.3 μM, respectively). Ribocyclophane E (**5**) showed no antiproliferative activity against either cell line at 25 μM, corroborating the findings of Preisitsch et al. that an unclosed [7.7]paracyclophane core structure does not retain antiproliferative activity.[15] Ribocyclophanes A and B and cylindrocyclophane D all had modest activity against the two cell lines, as shown in Supporting Information S18. Interestingly, the large glycone moieties do not seem to change the antiproliferative activity, as ribocyclophane D has similar activity levels to smaller [7.7]paracyclophanes such as the merocyclophanes.[8,11]

DOI: 10.1021/acs.jnatprod.7b00954
J. Nat. Prod. XXXX, XXX, XXX−XXX

Table 2. NMR Spectroscopic Data of Ribocyclophanes B (2) and C (3) in MeOH-d_4

	ribocyclophane B (2)		ribocyclophane C (3)	
no.	δ_C,[a,b] type	δ_H[b], mult. (J in Hz)	δ_C,[a,b] type	δ_H[b], mult. (J in Hz)
1	88.5, CH	3.65, d (10.2)	88.4, CH	3.66, d (10.2)
2	40.1, CH	1.66, m	40.1, CH	1.66, m
3	33.4, CH_2	0.65, m	33.3, CH_2	0.66, m
		0.76, m		0.79, m
4	28.6, CH_2	0.83, m	28.6, CH_2	0.81, m
		1.42, m		1.43, m
5	29.0, CH_2	0.72, m	29.3, CH_2	0.74, m
		0.95, m		0.97, m
6	33.9, CH_2	1.32, m	34.0, CH_2	1.32, m
		2.04, m		2.00, m
7	35.4, CH	3.16, m	35.4, CH	3.11, m
8	116.1, C		114.7, C	
9	157.7, C		156.9, C	
10	103.5, CH	6.24, s	106.5, CH	6.02, s
11	142.2, C		139.4, C	
12	107.6, CH	6.07, s	108.5, CH	5.97, s
13	156.0, C		155.7, C	
14	80.2, CH	3.74, d (9.6)	44.3, CH_2	1.81, t (12.6)
				2.61, dd 13.2, 3.6)
15	40.7, CH	1.56, m	35.4, CH	1.57, m
16	33.4, CH_2	0.65, m	35.3, CH_2	0.62, m
		0.76, m		1.01, m
17	28.6, CH_2	0.83, m	28.8, CH_2	0.81, m
		1.42, m		1.34, m
18	29.0, CH_2	0.72, m	29.3, CH_2	0.74, m
		0.95, m		0.97, m
19	33.9, CH_2	1.32, m	34.0, CH_2	1.32, m
		2.04, m		2.00, m
20	35.4, CH	3.16, m	35.4, CH	3.16, m
21	116.1, C		116.4, C	
22	157.7, C		157.2, C	
23	103.7, CH	6.20, s	103.9, CH	6.20, s
24	140.4, C		140.3, C	
25	107.8, CH	6.09, s	107.6, CH	6.09, s
26	155.0, C		155.7, C	
27	33.3, CH_2	1.47, m	33.3, CH_2	1.48, m
		1.95, m		1.94, m
28	30.2, CH_2	1.04, m	30.3, CH_2	1.06, m
		1.17, m		1.17, m
29	22.4, CH_2	1.19, m	22.3, CH_2	1.20, m
		1.29, m		1.29, m
30	13.1, CH_3	0.79, t (7.2)	13.1, CH_3	0.82, t (7.2)
31	33.3, CH_2	1.47, m	33.3, CH_2	1.48, m
		1.95, m		1.94, m
32	30.2, CH_2	1.04, m	30.3, CH_2	1.06, m
		1.17, m		1.17, m
33	22.4, CH_2	1.19, m	22.3, CH_2	1.20, m
		1.29, m		1.29, m
34	13.1, CH_3	0.79, t (7.2)	13.3, CH_3	0.79, t (7.2)
35	15.4, CH_3	1.05, d (7.2)	15.4, CH_3	1.05, d (6.6)
36	15.4, CH_3	1.06, d (6.6)	19.3, CH_3	0.95, d (6.6)
1'	103.0, CH	4.85, d (2.4)	103.0, CH	4.85, d (2.4)
2'	71.1, CH	3.73, brs	71.1, CH	3.73, brs
3'	65.2, CH	3.70, t (3.0)	65.3, CH	3.70, t (3.0)
4'	70.1, CH	3.60, brs	70.0, CH	3.59, brs
5'	63.9, CH_2	3.20, dd (12.6, 2.4)	64.0, CH_2	3.20, dd (12.6, 2.4)
		3.31, overlapped		3.31, overlapped

[a]Assigned from the HSQC and HMBC spectra. [b]Recorded at 600 MHz.

EXPERIMENTAL SECTION

General Experimental Procedures. Optical rotations were measured on a PerkinElmer 241 polarimeter. ECD spectra were recorded on a Jasco J-710 ECD spectrometer. UV and IR spectra were recorded on a Shimadzu UV2401 UV spectrometer and a Thermo Nicolet 6700 FT-IR spectrometer, respectively. 1D and 2D NMR spectra including ^{1}H NMR, COSY, TOCSY, HSQC, HMBC, and T-ROESY spectra were obtained on a Bruker Avance 600 MHz NMR spectrometer with a 5 mm CPTXI Z-gradient probe, whereas a Bruker Avance II 900 MHz NMR spectrometer with a 5 mm ATM CPTCI Z-gradient probe was used to acquire the DEPT-Q spectra. ^{1}H and ^{13}C NMR chemical shifts were referenced to the DMSO-d_6 solvent signals (δ_H 2.49 and δ_C 39.7, respectively) or MeOH-d_4 solvent signals (δ_H 3.31 and δ_C 49.15, respectively). A mixing time of 60 ms was set for the TOCSY experiment and 200 ms for the T-ROESY experiment. The HMBC spectrum was recorded with the average $^3J_{CH}$ of 8 Hz, and the HSQC spectrum was measured with the average $^1J_{CH}$ of 145 Hz. HRESIMS and LC-MS data were obtained on a Shimadzu IT-TOF LC-MS spectrometer.

Biological Material. *Nostoc* sp. (UIC 10279) was isolated from a sample collected in the southwest suburbs of Chicago near the town of Joliet, Illinois. The unialgal strain (UIC 10279) was produced through micropipet isolation techniques.[20] Taxonomic identification of the strain UIC 10279 was carried out using a partial 16S rRNA gene sequence (GenBank Accession No. JX962720; see SI, S2). *Nostoc* sp. (UIC 10366) was isolated from a sample collected in the northwest suburbs of Chicago near the town of Elgin, Illinois, through micropipet isolation.[20] Taxonomic identification of the strain UIC 10366 was carried out using a partial 16S rRNA gene sequence (GenBank Accession No. MF622942; see SI, S2). Both strains were cultured in four 2.8 L Fernbach flasks each containing inorganic Z media (4 × 2 L) with sterile aeration.[18] Cultures were illuminated with fluorescent lamps at 1.03 klx with an 18/6 h light/dark cycle. The temperature of the culture room was maintained at 22 °C. After 7 weeks, the biomasses were harvested by centrifugation and then freeze-dried.

Extraction and Isolation. The freeze-dried cells were each extracted with CH_2Cl_2–MeOH (1:1 v/v) three times and concentrated in vacuo to yield organic extracts (0.5 g of UIC 10279 and 0.65 g of UIC 10366). The resulting extracts were fractionated using Diaion HP-20 resin with an increasing amount of iPrOH in H_2O. The fractions eluting at 50% and 60% iPrOH were found to be active in the antiproliferative assay against MDA-MB-435 cells (95% and 97% at 25 μg/mL, respectively). HPLC-based activity profiling of the active fractions, which associates the HPLC chromatogram with biological activity, identified three active peaks for each strain. Dereplication of these peaks by LC-MS and ^{1}H NMR indicated these peaks to be new cyclophanes with the molecular weights of 848, 758, 716, and 700 Da. The fractions containing active peaks were combined and subjected to reversed-phase HPLC (Varian C_8 column, 10 mm × 250 mm, 3 mL/min) eluting with a gradient using aqueous MeOH from 60% to 80% over 40 min which led to the isolation of ribocyclophanes A (**1**, 15 mg, 0.5%), B (**2**, 3 mg, 0.1%), and C (**3**, 10 mg, 0.3%) from UIC 10279 and ribocyclophanes D (**4**, 15 mg, 0.5%) and E (**5**, 1 mg, > 0.1%) and cylindrocyclophane D (**6**, 6 mg, 0.2%) from UIC 10366.

Ribocyclophane A (1): white, amorphous powder; $[\alpha]^{25}_D$ −6 (*c* 0.12, MeOH); UV (MeOH) λ_{max} (log ε) 208 (4.41), 223 (3.88), 276 (3.13) nm; ECD (MeOH 1.0 mM) λ_{max} ($\Delta\varepsilon$) 208 (2.87), 224 (1.27), 282 (1.04) nm; IR (neat) ν_{max} 3365, 2930, 2857, 1628, 1432, 1381, 1321 cm^{-1}; ^{1}H and ^{13}C NMR, COSY, and HMBC data, Table 1; HRESIMS *m*/*z* 847.4894 $[M - H]^-$ (calcd for $C_{46}H_{71}O_{14}$, 847.4844).

DOI: 10.1021/acs.jnatprod.7b00954
J. Nat. Prod. XXXX, XXX, XXX−XXX

Table 3. NMR Spectroscopic Data of Ribocyclophanes D (4) and E (5) in MeOH-d_4

	ribocyclophane D (4)		ribocyclophane E (5)	
no.	δ_C,[a] type	δ_H,[c] mult. (J in Hz)	δ_C,[b] type	δ_H,[c] mult. (J in Hz)
1	90.1, CH	3.65, d (10.0)	87.6, CH	4.0, m
2	41.7, CH	1.64, m	40.4, CH	1.77, m
3	34.9, CH_2	0.65, m	33.9, CH_2	0.97, m
		0.76, m		1.26, m
4	30.0, CH_2	0.84, m	22.7, CH_2	1.32, m
		1.43, m		
5	30.8, CH_2	0.7, m	27.6, CH_2	1.33, m
		0.94, m		1.44, m
6	35.5, CH_2	1.33, m	39.4, CH_2	1.54, m
		2.03, m		1.62, m
7	37.0, CH	3.16, m	65.1, CH	3.83, m
8	118.7, C		102.7, CH	6.15, s
9	159.0, C		159.9, C	
10	109.6, CH	6.13, s	106.0, CH	6.17, s
11	139.3, C		144.1, C	
12	105.3, CH	6.18, s	106.0, CH	6.17, s
13	157.1, C		159.9, C	
14	83.6, CH	5.0, d (10.4)	80.8, CH	5.4, m
15	40.2, CH	1.77, m	39.9, CH	1.79, m
16	34.6, CH_2	0.71, m	30.6, CH_2	1.29, m
		0.78, m		
17	29.8, CH_2	0.84, m	29.8, CH_2	1.05, m
		1.43, m		1.34, m
18	30.7, CH_2	0.7, m	29.6, CH_2	1.09, m
		0.94, m		
19	35.4, CH_2	1.33, m	34.5, CH_2	1.47, m
		2.03, m		1.92, m
20	37.0, CH	3.16, m	36.4, CH	3.19, m
21	117.8, C		118.2, C	
22	159.0, C		158.3, C	
23	105.5, CH	6.2, s	107.3, CH	6.22, br
24	142.1, C		141.9, C	
25	109.2, CH	6.08, s	107.3, CH	6.22, br
26	157.1, C		158.3, C	
27	35.0, CH_2	1.49, m	39.4, CH_2	1.6, m
		1.91, m		1.68, m
28	31.8, CH_2	1.05, m	27.6, CH_2	1.29, m
		1.17, m		1.34, m
29	24.0, CH_2	1.19, m	23.4, CH_2	1.27, m
		1.29, m		1.33, m
30	14.8, CH_3	0.79, t (7.3)	14.3, CH_3	0.92, t (7.3)
31	34.8, CH_2	1.49, m	34.5, CH_2	1.5, m
		1.95, m		1.94, m
32	31.9, CH_2	1.05, m	31.7, CH_2	1.07, m
		1.17, m		1.17, m
33	24.1, CH_2	1.22, m	23.8, CH_2	1.22, m
		1.29, m		1.30, m
34	14.7, CH_3	0.82, t (7.3)	15.1, CH_3	0.82, t (7.2)
35	17.0, CH_3	1.05, d (6.4)	16.5, CH_3	0.99, d (6.5)
36	16.7, CH_3	0.96, d (6.4)	14.8, CH_3	0.85, d (6.5)
37	172.6, C		173.1, C	
38	21.3, CH_3	2.0, s	21.2, CH_3	2.07, s
1'	104.5, CH	4.85, d (2.0)	103.8, CH	4.89, br
2'	72.8, CH	3.72, brs	72.6, CH	3.76, br
3'	67, CH	3.7, t (3.2)	66.9, CH	3.78, br
4'	71.6, CH	3.6, brs	71.3, CH	3.67, br
5'	65.7, CH_2	3.2, dd (12.3, 2.5)	65.6, CH_2	3.32, overlapped
		3.32, overlapped		3.47, overlapped

[a]Assigned from the DEPT-Q spectrum acquired at 226 MHz. [b]Assigned from HSCQ and HMBC spectra. [c]Recorded at 900 MHz.

Spectroscopic data of **1** isolated from UIC 10366 were identical to those from UIC 10279.

*Ribocyclophane B (**2**):* white, amorphous powder; $[\alpha]^{25}_D$ −6 (*c* 0.07, MeOH); UV (MeOH) λ_{max} (log ε) 207 (4.10), 221 (3.65), 275 (2.90) nm; ECD (MeOH 0.7 mM) λ_{max} ($\Delta\varepsilon$) 208 (1.62), 222 (0.99), 284 (0.86) nm; IR (neat) ν_{max} 3378, 2930, 2858, 1631, 1469, 1432, 1372 cm^{-1}; ^1H and ^{13}C NMR data, Table 2; HRESIMS *m*/*z* 715.4471 $[M - H]^-$ (calcd for $C_{41}H_{63}O_{10}$, 715.4421).

*Ribocyclophane C (**3**):* white, amorphous powder; $[\alpha]^{25}_D$ +6 (*c* 0.16, MeOH); UV (MeOH) λ_{max} (log ε) 209 (4.54), 223 (4.03), 275 (3.23) nm; ECD (MeOH 0.7 mM) λ_{max} ($\Delta\varepsilon$) 211 (2.59), 224 (1.44), 282 (2.00) nm; IR (neat) ν_{max} 3382, 2926, 2856, 1691, 1620, 1592, 1431, 1369 cm^{-1}; ^1H and ^{13}C NMR data, Table 2; HRESIMS *m*/*z* 699.4533 $[M - H]^-$ (calcd for $C_{41}H_{63}O_9$, 699.4472).

*Ribocyclophane D (**4**):* white, amorphous powder; $[\alpha]^{25}_D$ −3 (*c* 0.14, MeOH); UV (MeOH) λ_{max} (log ε) 208 (4.38), 220 (3.85), 280 (3.05) nm; ECD (MeOH 1.0 mM) λ_{max} ($\Delta\varepsilon$) 211(2.82), 228 (1.21), 284 (0.9); IR (neat) ν_{max} 3380, 2931, 2862, 1625, 1433, 1372, 1256 cm^{-1}; ^1H and ^{13}C NMR data, Table 3; HRESIMS *m*/*z* 757.4548 $[M - H]^-$ (calcd for $C_{43}H_{65}O_{11}$, 757.4526).

*Ribocyclophane E (**5**):* white, amorphous powder; $[\alpha]^{25}_D$ +7 (*c* 0.14, MeOH); UV (MeOH) λ_{max} (log ε) 211 (3.82), 223 (3.61), 278 (2.98) nm; ECD (MeOH 0.7 mM) λ_{max} ($\Delta\varepsilon$) 208 (2.12), 226 (1.12), 277 (−0.8); IR (neat) ν_{max} 3405, 2930, 2858, 1567, 1426, 1387, 1257, 830 cm^{-1}; ^1H and ^{13}C NMR data, Table 3; HRESIMS *m*/*z* 793.4310 $[M - H]^-$ (calcd for $C_{43}H_{66}ClO_{11}$, 793.4293).

Single-Crystal X-ray Crystallographic Analysis of 1. A small single crystal, roughly 10 × 10 × 30 μm, was encased in Paratone-N oil and cooled to 100 K in a nylon loop. Data were collected at the Advanced Photon Source, LS-CAT, sector 21, on a MAR 300 mm CCD detector. A total of 240 images of width 1° were collected at a crystal-to-detector distance of 91 mm and wavelength 0.77 Å, to a resolution of 0.8 Å. The images were indexed, and the intensities were integrated and scaled with XDS.[21] The unit cell is monoclinic, space group $P2_1$, with two molecules in the asymmetric unit and eight disordered MeOH molecules. The structure was solved by SHELXS and refined with SHELXL.[22] Crystal data: $2C_{46}H_{72}O_{14}{\cdot}8C_2H_6O$, monoclinic, space group $P2_1$ (No. 4), a = 10.752(2) Å, b = 34.601(4) Å, c = 16.762(2) Å, β = 90.480(8)°, V = 6235.7(16) Å^3, Z = 4, D_c = 1.10, μ = 0.081, $F000$ = 2256. Reflections collected/unique = 55 588/23 169 (R_{int} = 0.0514), final R1 = 0.0996, wR2 = 0.2478 for reflections with $I > 2\sigma I$; R1 = 0.1063, wR2 = 0.2552 for all reflections; goodness-of-fit = 1.019 for all unique data. Bijvoet analysis: Flack x = −0.4(6), Parsons z = −0.24(15), probability P2(true) = 1.000. Crystallographic data (ID entry CCDC 898167) have been deposited in the Cambridge Crystallographic Data Centre.

Acid Hydrolysis of 1. Approximately 5 mg of **1** was hydrolyzed using 1 N HCl (1 mL) at 100 °C for 1 h. The resulting hydrolysate was air-dried and extracted with H_2O and EtOAc to yield the H_2O (1.3 mg) and EtOAc (3.9 mg) fractions. The negative specific rotation observed for the H_2O fraction suggested the sugar moiety to be D-ribopyranose: $[\alpha]^{25}_D$ −9 (*c* 0.13, H_2O). Reversed-phase HPLC of the EtOAc fraction (C_{18}, 60−80% aqueous MeOH) yielded the pure aglycone moiety (0.5 mg; HRESIMS *m*/*z* 583.4113 $[M - H]^-$). The ECD spectrum of the aglycone moiety displayed negative Cotton effects at 230 and 280 nm, indicating the same absolute configuration as that reported for cylindrocyclophane A.[6]

Antiproliferative Assay. The human melanoma cell line MDA-MB-435 and human breast cancer cell line MDA-MB-231 were purchased from the American Type Culture Collection. The cells were

DOI: 10.1021/acs.jnatprod.7b00954
J. Nat. Prod. XXXX, XXX, XXX−XXX

propagated at 37 °C in 5% CO_2 in RPMI 1640 medium supplemented with fetal bovine serum (10%), penicillin (100 units/mL), and streptomycin (100 μg/mL). Cells in log phase growth were harvested by trypsinization. A total of 5000 cells were seeded per well of a 96-well plate and incubated overnight at 37 °C in 5% CO_2. Samples dissolved in DMSO were then sequentially diluted and added to the appropriate wells (total volume 100 μL). Each compound was tested at the following concentrations (μg/mL): 25, 5.0, 1.0, 0.2, and 0.04. The cells were incubated in the presence of test substance for 96 h at 37 °C and evaluated for viability with a commercial absorbance assay (CellTiter 96 AQ_{ueous} One Solution cell proliferation assay, Promega Corp). Activity was expressed as the percentage of viable cells present relative to the negative (solvent) control. The positive control was vinblastine tested at 1 ng/mL, which had 49% viable cells after treatment.

■ ASSOCIATED CONTENT

Supporting Information

The Supporting Information is available free of charge on the ACS Publications website at DOI: 10.1021/acs.jnatprod.7b00954.

Taxonomic identification and phylogenetic tree of UIC 10279 and UIC 10366 strains; ^{1}H NMR, COSY, HSQC, and HMBC spectra of **1**−**5**; DEPT-Q spectrum of **1** and **4**, ECD spectra of **1**−**5**, and antiproliferative data for **1**−**6** against MDA-MB-435 and MDA-MB-231 cancer cell lines (PDF)

Crystallographic data (CIF)

Crystallographic data (CIF)

■ AUTHOR INFORMATION

Corresponding Author

*Tel: +1-312-996-5583. Fax: +1-312-996-7107. E-mail: orjala@uic.edu.

ORCID

Hahk-Soo Kang: 0000-0001-9602-6042

Jimmy Orjala: 0000-0002-4420-2048

Present Address

[§]Department of Biomedical Sciences and Engineering, Konkuk University, Seoul 05029, Korea.

Author Contributions

[‖]D. S. May and H.-S. Kang contributed equally.

Notes

The authors declare no competing financial interest.

■ ACKNOWLEDGMENTS

This research was supported by PO1 CA125066 from NCI/NIH and T32AT00753, The Office of the Director, National Institutes of Health (OD) National Center for Complementary and Integrative Health (NCCIH) to D.S.M. We thank Dr. B. Ramirez from Center for Structural Biology at UIC for assistance with NMR experiments. LC-MS analysis was performed at UIC Research Resource Center (RRC) Mass Spectrometry Facility. We acknowledge the use of the Southeast Regional Collaborative Access Team (SER-CAT), beamline 22-BM, for data collection of these small crystals. Use of the Advanced Photon Source at Argonne National Laboratory was supported by the U.S. Department of Energy, Office of Science, Office of Basic Energy Sciences, under Contract No. DE-AC02-06CH11357.

■ DEDICATION

Dedicated to Susan Band Horwitz, of Albert Einstein College of Medicine, Bronx, NY, for her pioneering work on bioactive natural products.

■ REFERENCES

(1) Tan, L. T. *Phytochemistry* **2007**, *68*, 954−979.

(2) Van Wagoner, R. M.; Drummond, A. K.; Wright, J. L. C. *Adv. Appl. Microbiol.* **2007**, *61*, 89−217.

(3) Chlipala, G. E.; Mo, S.; Orjala, J. *Curr. Drug Targets* **2012**, *12*, 1654−1673.

(4) Moore, B. S.; Chen, J.; Patterson, G. M. L.; Moore, R. E. *Tetrahedron* **1992**, *48*, 3001−3006.

(5) Chen, J. L.; Moore, R. E.; Patterson, G. M. L. *J. Org. Chem.* **1991**, *56*, 4360−4364.

(6) Bui, H. T. N.; Jansen, R.; Pham, H. T. L.; Mundt, S. *J. Nat. Prod.* **2006**, *69*, 1379−1383.

(7) Chlipala, G. E.; Sturdy, M.; Krunic, A.; Lantvit, D. D.; Shen, Q.; Porter, K.; Swanson, S. M.; Orjala, J. *J. Nat. Prod.* **2010**, *73*, 1529−1537.

(8) Kang, H. S.; Santarsiero, B. D.; Kim, H.; Krunic, A.; Shen, Q.; Swanson, S. M.; Chai, H.; Kinghorn, A. D.; Orjala, J. *Phytochemistry* **2012**, *79*, 109−115.

(9) Preisitsch, M.; Harmrolfs, K.; Pham, H. T.; Heiden, S. E.; Füssel, A.; Wiesner, C.; Pretsch, A.; Swiatecka-Hagenbruch, M.; Niedermeyer, T. H.; Müller, R.; Mundt, S. *J. Antibiot.* **2015**, *68*, 16510.1038/ja.2014.118.

(10) Luo, S.; Kang, H.-S.; Krunic, A.; Chlipala, G. E.; Cai, G.; Chen, W.-L.; Franzblau, S. G.; Swanson, S. M.; Orjala, J. *Tetrahedron Lett.* **2014**, *55*, 686−689.

(11) May, D. S.; Chen, W.; Lantvit, D. D.; Zhang, X.; Krunic, A.; Burdette, J. E.; Eustaquio, A.; Orjala, J. *J. Nat. Prod.* **2017**, *80*, 1073−1080.

(12) Bobzin, S.; Moore, R. *Tetrahedron* **1993**, *49*, 7615−7626.

(13) Nakamura, H.; Hamer, H. a.; Sirasani, G.; Balskus, E. P. *J. Am. Chem. Soc.* **2012**, *134*, 18518−18521.

(14) Nakamura, H.; Wang, J. X.; Balskus, E. P. *Chem. Sci.* **2015**, *6*, 3816−3822.

(15) Preisitsch, M.; Niedermeyer, T. H. J.; Heiden, S. E.; Neidhardt, I.; Kumpfmüller, J.; Wurster, M.; Harmrolfs, K.; Wiesner, C.; Enke, H.; Müller, R.; Mundt, S. *J. Nat. Prod.* **2016**, *79*, 106−115.

(16) Nakamura, H.; Schultz, E. E.; Balskus, E. P. *Nat. Chem. Biol.* **2017**, *13*, 916−921.

(17) Preisitsch, M.; Heiden, S. E.; Beerbaum, M.; Niedermeyer, T. H. J.; Schneefeld, M.; Herrmann, J.; Kumpfmüller, J.; Thürmer, A.; Neidhardt, I.; Wiesner, C.; Daniel, R.; Müller, R.; Bange, F. C.; Schmieder, P.; Schweder, T.; Mundt, S. *Mar. Drugs* **2016**, *14*, 21.

(18) Falch, B. S.; Konig, G. M.; Wright, A. D.; Sticher, O.; Angerhofer, C. K.; Pezzuto, J. M.; Bachmann, H. *Planta Med.* **1995**, *61*, 321−328.

(19) Vijayalakshmi, K. S.; Rao, V. S. R. *Carbohydr. Res.* **1972**, *22* (2), 413−424.

(20) Chlipala, G.; Mo, S.; Carcache de Blanco, E. J.; Ito, A.; Bazarek, S.; Orjala, J. *Pharm. Biol.* **2009**, *47*, 53−60.

(21) Kabsch, W. *J. Appl. Crystallogr.* **1993**, *26*, 795−800.

(22) Sheldrick, G. M. *Acta Crystallogr., Sect. A: Found. Crystallogr.* **2008**, *64*, 112−122.

DOI: 10.1021/acs.jnatprod.7b00954
J. Nat. Prod. XXXX, XXX, XXX−XXX